15TH IEA HEAT PUMP CONFERENCE
MAY 26–29, 2026 | HOFBURG
VIENNA 2026
DECARBONISATION THROUGH INNOVATION

AI-Based Predictive Controller for Residential Heat Pumps: From Simulation to a Season-Long Field Trial

Lilli Frison*[1], Simon Gölzhäuser[2], Danny Günther[2], Nicolas Réhault[2]

[1] *Systems Control and Optimization Laboratory, University of Freiburg, Freiburg, Germany*
[2] *Fraunhofer Institute for Solar Energy Systems ISE, Freiburg, Germany*

Abstract

Heat pumps are essential for building decarbonisation, yet the fixed heating-curve controllers supplied with most units perform poorly under variable operating conditions. This study presents a vendor-independent neural-network controller that can be retrofitted to existing HPs through standard 0–10 V or Modbus interface, replacing the static control curve with a predictive, optimisation-in-the-loop strategy. A lightweight Transformer model forecasts indoor air temperature several hours ahead using existing heat-pump sensor data, including indoor, outdoor, return, and supply temperatures. A real-time capable optimiser selects the supply-water temperature that minimises a weighted sum of thermal discomfort and compressor energy, thus realising model-predictive-control benefits without requiring a physical plant model or cloud infrastructure. Simulations on nine German buildings from the TABULA database indicate electricity savings of up to 15 % and a seasonal COP increase of up to 0.3, while the duration of comfort violations is halved relative to a manufacturer standard heating curve. A field trial during the 2024/25 heating season in a renovated single-family house (radiators, 11 kW HP) confirmed a seasonal COP rise of around 0.2, an 8 – 11 % reduction in daily electricity demand, and a decrease in mean absolute comfort deviation. Over a 180-day season these figures correspond to approximately 387 kWh and 23 kg CO_2 saved per building.

Selection and/or peer-review under the responsibility of the organizers of the 15th IEA Heat Pump Conference 2026.

Keywords: heat pumps; retrofit; artificial intelligence; Transformer model; model predictive control; building decarbonisation

1. Introduction

1.1. Motivation

Reducing greenhouse-gas emissions from buildings is one of the most pressing challenges in climate policy. Space heating and domestic hot-water production represent a major portion of emissions within buildings—which in turn produce about one-fifth of global greenhouse-gas emissions [1], largely because they rely on combustion of fossil fuels or direct electrical resistance heating. Electric resistance heating requires substantially more electricity than heat pumps to deliver the same useful heat, leading to higher system-level electricity demand and, depending on the grid mix, higher associated emissions and operating costs. Electric heat pumps offer a promising solution because they move heat rather than generate it. Modern residential units can transfer three to four times more thermal energy than they consume as electricity and consequently reduce carbon dioxide emissions by 38–58 % relative to gas furnaces when the electricity mix is moderately clean [2]. Achieving these goals requires not only deploying millions of heat pumps but also operating them efficiently.

Residential heat pumps are typically controlled by a heating curve that specifies the supply-water temperature as a function of the outdoor temperature. The heating curve is characterised by a slope and an offset. The slope indicates how steeply the flow temperature increases when the outdoor temperature drops and the offset allows a uniform shift of the curve. Manufacturers provide default values based on typical buildings, but the optimal settings depend on insulation, radiator type and occupancy. If the slope is too high,

* Corresponding author. *E-mail address:* lilli.frison@imtek.uni-freiburg.de

unnecessary high flow temperatures increase heat losses and reduce efficiency; if too low, the building may not warm adequately. Adjusting the heating curve requires manual intervention and often an expert, yet even an optimally set curve cannot account for internal gains, solar radiation, wind or short-term weather fluctuations. Static control strategies and lack of real-time adaptability mean that traditional HVAC systems often waste energy and compromise comfort.

1.2. Related work

1.2.1. Deep Neural Network Predictive Control for Heat Pumps

Recent studies leverage neural networks to improve predictive control of residential heat pump systems. One approach is to use deep learning models for forecasting and control within a model predictive control (MPC) framework [3]. Stoffel, Berktold and Müller (2024) proposed a real-life data-driven MPC framework that automatically translates different machine-learning models into an optimisation syntax for efficient MPC [4]. Frison and Gölzhäuser (2024) developed an attention-based encoder–decoder long short-term memory (LSTM) network (drawing on Transformer architectures) to serve as a predictive model for heating control [5]. Although primarily demonstrated in simulation, such advanced neural network models hold promise for accurate, adaptive predictive control in real homes.

Another line of work uses imitation learning to derive lightweight controllers from an offline computed MPC. Maier et al. (2024) proposed an approximate MPC strategy where a neural network policy is trained to mimic optimal MPC behaviour for a two-zone residential heat pump system [6]. In their study, a deep artificial neural network (NN) served as a functional approximator, replacing real-time optimisation. After careful feature selection, the learned NN controller outperformed a conventional rule-based thermostat, yielding up to 33 % cost savings and a 70 % reduction in discomfort relative to the baseline control, while requiring only ~15 % of the computation time of full MPC. Dengiz and Kleinebrahm (2024) underscores the potential of imitation learning to deliver fast, transferable controllers for demand-response heat pump operation while maintaining comfort [7]. Such works demonstrate that data-driven controllers (NN or random forest) can capture much of MPC's performance benefits (in energy cost and comfort) at a fraction of the runtime cost. Such approaches bridge the gap between high-performance MPC and practical deployability by offloading the heavy optimisation to an offline training phase, resulting in a fast runtime controller. Frison et al. (2021) confirm the performance of imitation learning for heat pump temperature control using neural networks such as convolutional neural network (CNN) and recurrent neural network (RNN) in a hardware-in-the loop experiment with a real heat pump [15].

1.2.2. Reinforcement Learning for Residential Heat Pump Control

Reinforcement learning (RL) has emerged as a powerful paradigm for optimising heat pump operations under dynamic conditions. Several works have applied RL agents to control HVAC heat pumps with objectives like energy efficiency and cost savings. Early simulation studies indicated that RL-based HVAC control policies can adapt to varying conditions in residential houses [8, 11]. In recent years, more sophisticated and practical implementations have been explored. Svetozarević et al. (2022) developed a deep deterministic policy gradient (DDPG) agent to jointly control a radiant floor heating system (supplied by a heat pump) and coordinate with an electric vehicle charger [9]. The RL agent was trained offline on a recurrent neural network simulator of a residential module and then tested in both simulation and a lab setup. It achieved about 11–21 % reduction in operating cost compared to a standard baseline strategy, demonstrating the potential of RL to optimise heat pump usage and energy arbitrage (e.g. leveraging time-of-use electricity prices) without explicit building models. Another study by Montazeri et al. (2025) applied a fully data-driven RL controller, enhanced with a physically consistent model of building dynamics, to a high-performance building testbed [10]. Using DDPG and modular control structures, they reported 26–32 % heating energy savings versus the measured baseline, without compromising thermal comfort. These results underscore that model-free RL can learn near-optimal heat pump control policies that save substantial energy while respecting comfort constraints, at least in well-modelled environments.

Researchers have begun to evaluate RL approaches in real buildings. In a noteworthy field trial, Mulayim et al. (2025) conducted a month-long head-to-head comparison of RL and MPC in an occupied single-family house with an air-to-air heat pump and electric resistance backup [12]. The RL controller was a model-based algorithm that learned a dynamics model and reward function automatically, while the MPC was expertly tuned with a physics-based model. Both advanced controllers were benchmarked against the home's conventional PID thermostat. Results showed the RL agent achieved ~22 % HVAC energy savings relative to the baseline, comparable to the MPC's 20 % savings. However, RL's policy led to slightly higher average discomfort and delivered a lower comfort-normalised efficiency improvement, illustrating that careful reward design and hybrid methods may be needed to match MPC's comfort performance and reliability.

Several researchers have begun exploring hybrid RL approaches to address safety and efficiency. For instance, constrained or safe RL algorithms (e.g. variants of soft actor-critic with safety layers) have been tested to enforce temperature limits and avoid discomfort during learning (Zhang et al., 2024 [13]). Benchmarking demonstrates improved data exploration, constraint satisfaction and performance compared to baseline algorithms including MPC.

1.2.3. Field trials of AI-enabled controllers (buildings, HVAC, HP)

Reliable field evidence for AI-enabled control of building systems remains limited. Most reported studies on MPC, RL or other AI-enabled control methods still rely on simulation or short-term pilots. Approaches range from pure reinforcement learning (RL) to hybrid MPC–ML methods. Reported energy or cost savings are relative to conventional control (e.g. PID thermostat or rule-based). Field tests on AI-enabled controllers that directly control heat pump operation, rather than merely adjusting zone or storage setpoints, are even rarer. Montazeri et al. (2025) [10] presented a modular deep-RL controller based on the Deep Deterministic Policy Gradient (DDPG) algorithm, validated both in simulation and in the Empa NEST building. The controller was transferable across rooms and achieved average energy savings of around 13 %—up to 17 % in some cases—compared with transfer-learning baselines, and about 26 % (up to 32 %) compared with rule-based control, without compromising thermal comfort. Mulayim et al. (2025) [12] conducted a one-month field deployment comparing a model-based RL controller and an MPC controller in an occupied house equipped with a heat pump. The RL controller reduced energy use by roughly 22 % relative to the existing baseline, while MPC achieved about 20 %. When adjusted for comfort, MPC performed slightly better, underlining the trade-off between energy savings and comfort that still characterises RL in real-world operation. Pergantis et al. (2024) [14] investigated predictive setpoint scheduling for an air-to-air heat pump with electric-resistance backup in an occupied single-family house over about three months. The controller achieved roughly 19 % lower heating energy use and significantly reduced backup-heater demand, while occupant surveys confirmed acceptable comfort. Even less heat-pump-specific, a field trial was reported by Stoffel et al. (2024) [4], who evaluated a data-driven MPC scheme in two real-life cases: five office rooms with smart radiator valves and a test hall with an air-handling unit. The six-week deployment compared linear, neural-network, and Gaussian-process models. While not directly focused on heat-pump flow-temperature control, it illustrated that many field demonstrations still target zone or HVAC component control rather than end-to-end HP operation.

Overall, real-building studies of AI-enabled HP controllers remain scarce, short in duration, and fragmented across different control targets. The performance gains, however, depend strongly on experimental design, the way comfort is normalised and reference operation, so such results should be interpreted together with details on trial setup, occupant behaviour, and weather conditions.

1.3. Contributions

In this paper we present a vendor-independent, edge-AI retrofit controller that can be connected to most existing residential heat pumps without modifying refrigerant circuits or hardware. The controller uses a lightweight Transformer model to forecast indoor air temperature several hours ahead based on readily available sensor data and a real-time optimiser that minimises a weighted sum of thermal discomfort and compressor energy. The contributions of this work include:

1. A retrofit and software design that interfaces with standard 0–10 V or Modbus terminals to override the heating curve set-point.
2. A low-parameter Transformer model that runs on an embedded processor and forecasts the indoor air temperature using only the heat pump's built-in sensors.
3. A real-time optimisation algorithm that selects the supply-water temperature to minimise predicted discomfort and energy consumption over a rolling horizon.
4. A simulation study using nine archetype buildings representing different construction years and insulation standards in Germany.
5. A field trial during the 2024/25 heating season in a renovated single-family house.

The remainder of the paper is organised as follows: Section 2 describes the retrofit controller architecture and modelling approach. Section 3 presents simulation and field-trial results, which are discussed in Section 4. Conclusions and future work are summarised in Section 5.

2. Methods and approach

2.1. Retrofit hardware integration

Most modern residential heat pumps allow the supply-water temperature to be set via a voltage or digital input. The proposed controller can be implemented on an embedded board (e.g., a Raspberry Pi 4 Model B) connected via a digital-to-analogue converter to the heat pump’s 0–10 V input. Alternatively, when the heat pump offers Modbus communication, the controller writes the desired supply-water temperature directly via the Modbus register. The retrofit does not modify refrigerant components or compressor hardware; the heat pump’s native control continues to manage defrosting and protective functions. A fail-safe ensures that if the retrofit controller is disconnected, the heat pump reverts to its factory heating curve. Figure 1 illustrates the overall architecture. Sensor data from the heat pump—outdoor temperature, return and supply-water temperatures— and at least one reference sensor for indoor air temperature are fed into the Transformer-based neural network forecasting model. The model predicts the indoor temperature over a horizon of several hours (e.g. 4 up to 24). The real-time optimiser computes the supply-water temperature trajectory that minimises a cost function balancing comfort and energy. The first control action is sent to the heat pump, and the process repeats every timestep, e.g., 15 minutes.

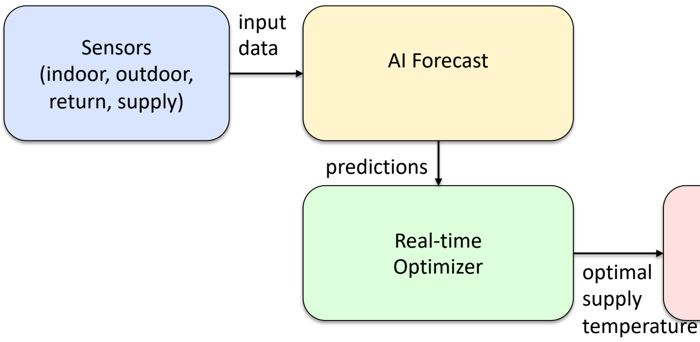

Figure 1: Block diagram of the AI-driven retrofit controller.

2.2. Neural network-based temperature forecasting

The forecasting model is based on a simplified Transformer architecture with LSTM neural networks for encoder and decoder. The input sequence comprises the last samples of indoor, outdoor, return and supply-water temperatures and the previous control inputs. After normalisation, the sequence is passed through positional encoding and several self-attention layers, see Figure 2. The output head produces a vector of predicted indoor temperatures. The model contains fewer than 50k parameters and can be executed in a few milliseconds per inference. It is trained offline using measured time series from the target building or from a representative archetype. The loss function is the mean squared error between predicted and observed indoor temperatures.

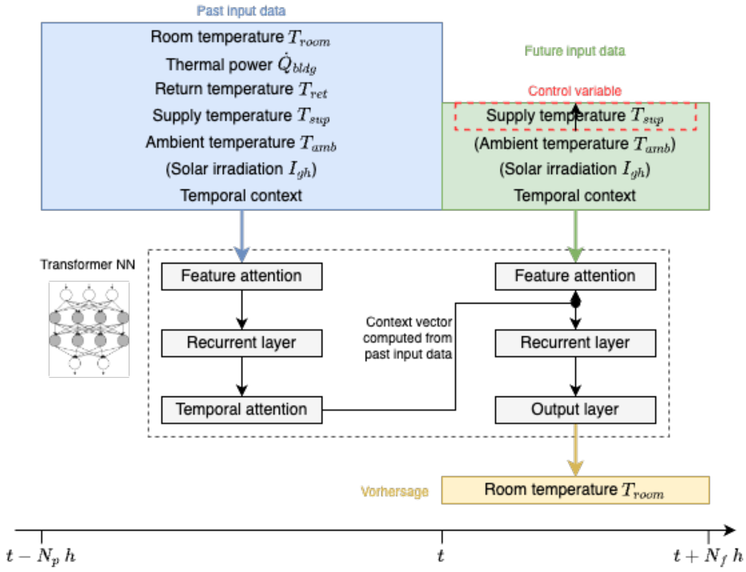

Figure 2: Overview of input data and neural network architecture for room temperature prediction.

2.3. Real-time optimisation formulation

At each control step t, the optimiser solves a finite-horizon optimal control problem that balances user comfort and energy efficiency. $y_t = T_{out,t}$ denote the predicted indoor (or outlet-side) temperature at future time step $t+1$, and let $u_t = T_{hp,t}$ denote the control input, i.e. the heat-pump supply-water temperature at time t. The objective is to determine the optimal control trajectory $\{T_{hp,t+1}, .., T_{hp,t+N}\}$ that minimises a weighted sum of the predicted comfort deviation and the compressor's electrical power consumption over the prediction horizon N.

$$min_{T_{hp}} \sum_{k=0}^{N} (T_{room,t+k} - T_{ref})^2 + c\, P_{el,t+k} \qquad \text{Minimize comfort deviation and HP power supply}$$

where the first term penalises deviations of the indoor temperature from the user-defined comfort setpoint T_{ref} and the second term penalises the electrical power consumed by the compressor. The weighting factor $c > 0$ determines the trade-off between comfort and energy efficiency.
The optimisation is subject to the following system dynamics and operational constraints:

$$T_{room,t+k+1} = f\left(T_{room,,t+k}, T_{hp,sup,k}, T_{amb,k}, p_k\right), \quad k = 0, .., N \qquad \text{Thermal building model with parameters p}$$

$$P_{el,k} = g\left(T_{hp,sup,,k}, T_{amb,k}, p_k\right), \quad k = 0, .., N \qquad \text{HP power model}$$

$$T_{room,t} = T_{room,,given}, \qquad \text{Initial condition}$$

$$T_{room,min} \leq T_{room,t+k} \leq T_{room,,max}, \quad k = 0, .., N \qquad \text{Output constraint}$$

$$T_{hp,sup,min} \leq T_{hp,sup,t+k} \leq T_{hp,sup,max}, k = 0, .., N \qquad \text{Control constraint}$$

Here f represents the building's thermal response to the heat-pump supply temperature and ambient conditions, while g describes the corresponding electrical power consumption. In discrete time, this problem is solved at each step using a quadratic programming (QP) solver based on predicted trajectories $(T_{out,t+k}, P_{el,t+k})$. Only the first control action $T_{hp,t}$ of the optimal sequence is applied to the heat pump. The optimisation is then repeated at the next time step in a receding-horizon fashion. If the optimiser fails to converge within a certain time, the controller reverts to the previous control value to ensure safe operation.

2.4. Simulation framework I4B for testing HP control strategies

The data that we used in this work to train, validate and test the proposed HP control strategy is obtained from a simulation framework provided by Fraunhofer ISE, called I4B. It simulates a simplified building with a single room which is heated by an underfloor heating system. The setup and functionality are explained in the subsequent paragraphs.

2.4.1. Thermal building behaviour

The building is defined by the following parameters: Living area, room height, transmission losses, ventilation losses, thermal capacity of the building as well as information about the windowed areas. We obtain the parameters for the buildings used in this project from the TABULA WebTool[1]. This tool provides information for generically specified buildings in European countries which are categorized by region, period of construction, state of renovation and building type. A HP is used in the simulation framework to heat the respective building. The heating system is defined in terms of HP type and refrigerant mass flow.

2.4.2. Heat pump model

The thermal power output of the heat pump, $\dot{Q}_{hp}$is determined from the supply and return temperatures $T_{\mathrm{hp}}$and $T_{\mathrm{hp,ret}}$ and the typically constant mass flow rate $\dot{m}_{hp}$ of the building's heat emission system.
To evaluate the heat pump's efficiency, it is noted that the device transfers heat from a lower to a higher temperature level using mechanical work—a process idealized by the reversible Carnot cycle. The Carnot coefficient of performance is determined by the temperature lift between the heat source and the heat sink, expressed in absolute temperatures (K), and represents the theoretical upper limit of heat-pump efficiency: $COP_{carnot} = \frac{T_{sink}}{T_{\mathrm{sink}}-T_{\mathrm{source}}}$.
In practice, heat pumps operate with losses, and their actual coefficient of performance (COP) is reduced by the exergetic efficiency η_{hp}:

$$COP = \eta_{hp} COP_{carnot}$$

Modern air-to-water heat pumps typically reach an exergetic efficiency of around $\eta_{hp} \approx 0.45$.
Rather than assuming a constant efficiency factor, the dependence of the COP on the source and sink temperatures (such as $T_{\mathrm{hp,sup}}$ and T_{amb}) is often approximated by a second-order polynomial fitted to manufacturer data.
Electric power is computed from heat and COP as follows:

$$P_{\mathrm{el}} = \frac{\dot{Q}_{hp}}{COP} = \frac{\dot{m}_w \, c_{p,w} (T_{\mathrm{hp,sup}} - T_{\mathrm{amb}})}{COP}$$

where $\dot{m}_w$ is the water mass flow rate and $c_{p,w}$ is the specific heat capacity of water.

2.4.3. Solar and internal heat gains

The online tool PVGIS[2] (Photovoltaic Geographical Information System) provides information about solar irradiation as well as expected photovoltaic system performance for a given location. The simulation framework calculates solar heat gains $\dot{Q}_{sol}$ based on the irradiation values. Additionally, also a profile for internal heat gains $\dot{Q}_{int}$ inside the building can be specified. These gains result from inhabitant's body heat as well as from heat emitted by electrical devices. The values for solar irradiation and the internal gain profile are combined in a disturbances profile of summed heat gains $\dot{Q}_{gains} = \dot{Q}_{sol} + \dot{Q}_{int}$.

2.4.4. Simplifications

The following simplifications are done in the simulation framework.

- Single zone building. I4B models one thermal zone representing the entire living area, heated via a hydronic underfloor loop by a heat pump (HP). No room-by-room control is simulated.
- Simplified heating system. The plant is a single air-to-water HP feeding one underfloor circuit. The only manipulated variable is the supply water temperature. Device-level behaviour (compressor, pump, valves) is abstracted by the HP model. No auxiliary/bivalent heater, buffer/storage tank, hydraulic separator, zone/mixing valves, PV coupling, demand-response interface, or domestic hot water (DHW) cycle is included. This yields exactly one control input for the single-zone setup.
- Constant mass flow. The mass flow in the heating circuit is fixed; the controller acts solely through ($T_{\mathrm{hp,sup}}$). Thermostatic effects or other flow-changing influences are neglected.
- Simplified HP model based on manufacturer's data. No defrosting mechanism.
- Internal gains fixed. Time-invariant internal gains are applied as $\dot{Q}_{int} = 5\ \frac{W}{m^2}$, of heated floor

[1] https://webtool.building-typology.eu
[2] https://joint-research-centre.ec.europa.eu/photovoltaic-geographical-information-system-pvgis_en

area (per DIN 4108-6[3]). Occupant presence and plug-load variability are not modelled.
- Reduced building/exogenous detail. The envelope is homogeneous (no thermal bridges beyond the lumped model), shading is not modelled, and sensors are ideal (no noise, no faults). Operation is limited to the heating season; active cooling and DHW are out of scope.
- Perfect weather forecast. Historical PVGIS weather series provide both past and "future" inputs to the forecasting model; by construction the forecast is perfect.
- Controller/solver scope. Safety limits and device protections are assumed to be enforced by the HP's internal controller; the optimisation only sets ($T_{\mathrm{hp,sup}}$) within admissible bounds at the simulation time step (5–60 min, depending on the run).

2.5. Simulation setup for evaluation

2.5.1. Data and settings
Nine reference buildings representing the German residential building stock were modelled using the TABULA project typology (archetypes from construction periods 1950–1985, 1986–1995 and 1996–2010, with detached, semi-detached and terraced house variants). The simulation environment couples a detailed thermal model of each building envelope with an air-to-water heat pump. The reference heat pump operates with a constant heating curve based on outdoor temperature. Internal gains, occupant schedules and weather data drive the building dynamics.
For each building archetype two control strategies are compared:
- Manufacturer heating curve (baselines**).** The supply-water temperature is calculated from the static heating curve provided by the manufacturer.
- AI-retrofit controller. The retrofit control described above replaces the heating-curve set-point. The Transformer model is trained on the first month of simulation data for each archetype; the optimiser horizon is 4 hours, and weights are tuned to achieve a comfort deviation within ±0.5 K. We consider two versions, one with exposure to weather forecast and one without.

2.5.2. Rule-based (heating curve) controller
To assess the performance of the adaptive AI-based heat pump (HP) control, results are compared against the rule-based heating curve controller implemented in the I4B framework. The heating curves are tuned in terms of their slope and their vertical offset. This is done by adjusting the parameters Y_{shift} (nominal supply/return temperature shift, slope) and Y_{offset} (vertical offset) of the I4B heating curve control. Two reference versions are used:
- Perfectly tuned heating curve (Rule-based tuned (RB-T))**:** optimized using both past and future data to achieve minimal comfort deviation. For each simulated building, heating curve parameters are tuned so that indoor temperatures stay as close as possible to the target setpoint, while ensuring the minimum negative comfort deviation satisfies $CD\downarrow_{min} \geq -1\,K.$
- Standard heating curve (Rule-based basic (RB-B)): representative of typical installations, adapted to the building type but not fine-tuned for the specific dataset.

2.6. Field trial

2.6.1. Test building

Figure 3 : Single-family house for field test

The field trial was conducted during the 2024/25 heating season in collaboration between the heat pump manufacturer Stiebel Eltron and Fraunhofer ISE. It took place in an inhabited building, which is a renovated single-family house with radiator heating near Hannover, Germany. The building (see Figure 3), constructed in 1980, insulated to energy-efficiency class B, has a heated floor area of 160 m² and uses radiators supplied by an 11 kW air-to-water heat pump installed in 2020. The occupant set-point is 21 °C for the test period but varied in previous periods.

[3] DIN V 4108-6:2003-06. Thermal protection and energy economy in buildings - part 6: Calculation of annual heat and energy use. 2003

2.6.2. Data selection and fair comparison

The retrofit controller was installed in October 2024 and operated continuously until April 2025. Data from the preceding heating season were used as baseline. Electricity consumption of the heat pump was measured with an energy meter and indoor air temperature at 15-minute intervals. Measurement data was available from October 2023 onwards, which was used to train the forecasting network in combination with synthetic simulation data. For the field test, the nighttime setback was disabled. The reference periods were selected based on comparable outdoor temperature conditions and high data quality. Direct comparison is challenging due to variations in nighttime setback and setpoint temperatures in the previous year. Initial short-term tests in the building identified necessary adaptations to the control and prediction modules, including feature engineering for forecast improvement, adjustments of the prediction horizon to 24 h and timestep to 15min. Subsequently, a one-week test phase and a seasonal test were conducted.
The seasonal tests cover several months of the 2024/25 heating season (November to March), excluding periods in which control adjustments were required. AI-based operation was compared against the standard controller. To ensure a fair comparison, we matched the datasets by mean ambient temperature, since ambient temperature has a strong impact on the achievable COP. For the one-week AI test (i), the reference period 01/11/23–30/01/24 was selected because it exhibits a similar average ambient temperature. For the seasonal tests (ii, iii), we selected a sufficient number of days from the 2023/24 heating season such that the resulting average ambient temperature matches the AI-operation period.

2.7. Evaluation metrics

To compare differently parametrized adaptive AI HP control algorithms against each other as well as against a traditional rule-based heating curve control, the following metrics are considered:

- Comfort deviation CD. The positive and negative deviation of the room temperatures T_{room} which the respective control method achieves from a given target room temperature T_{target}. We consider $CD\uparrow_{max}$, $\overline{CD\uparrow}$, $CD\downarrow_{min}$ and $\overline{CD\downarrow}$. The upwards arrow means that only positive deviations are considered for this metric, the downwards arrow accordingly denotes negative deviations (with respect to the target room temperature T_{target}).
- Energy consumption E_{el}. The total electrical energy that the HP consumed
- Coefficient of Performance COP. The average COP that the HP achieves.

3. Results

3.1. Simulation results

We compare two AI-based HP temperature controllers (with exposure to weather forecasts and without) against two heating-curve baselines: RB-B (briefly tuned, realistic) and RB-T (optimally tuned with full-year weather hindsight, unrealistic for deployment). The inputs for the AI-controllers are identical except that one variant uses a weather forecast and one does not. We evaluate simulation results across three archetypical TABULA single-family houses with different sizes, construction periods and renovation states. Results are summarized in Table 1. Both AI-based control algorithms cut electricity use versus RB-B by 6–15% and up to 10% versus RB-T, while increasing COP and tightening comfort around the setpoint. The forecasted AI-control yields the lowest energy use in two of three cases. Without forecasts it still beats RB-B and matches or approaches RB-T. Exemplary behaviour for the AI-control (with weather forecast) and heating curve control (RB-T) are shown in Figure 4 and Figure 5, respectively.

Table 1 : Simulation results for three buildings (single-family houses (SFH)) with different construction periods and renovation states.

Building (construction, renovation state, heating area)	Controller	E_{el} (kWh)	Saving vs RB-B	Saving vs RB-T	COP	Mean CD↑ (K)	Min CD↓ (K)
SFH 1949–1957,	RB-B	3427.76	—	—	4.12	0.94	−0.84
ENEV,	RB-T	3203.44	6.5 %	—	4.25	0.43	−0.97
111 m²	AI-control	3056.46	10.8 %	4.6 %	4.33	0.05	−0.80
	AI-control	3098.25	9.6 %	3.2 %	4.31	0.10	−3.04

Building (construction, renovation state, heating area)	Controller	E_{el} (kWh)	Saving vs RB-B	Saving vs RB-T	COP	Mean CD↑ (K)	Min CD↓ (K)
	(no forecast)						
SFH 1969–1978,	RB-B	11578.40	—	—	3.10	1.10	−0.46
State of construction	RB-T	10857.66	6.2 %	—	3.20	0.65	−0.97
173 m^2	AI-control	9948.30	14.1 %	8.4 %	3.33	0.05	−0.81
	AI-control (no forecast)	10098.98	12.8 %	7.0 %	3.29	0.20	−1.86
SFH 2010–2015,	RB-B	2003.30	—	—	4.60	1.40	−0.67
KfW	RB-T	1750.08	12.6 %	—	4.81	0.32	−0.98
187 m^2	AI-control	1709.47	14.7 %	2.3 %	4.90	0.17	−1.53
	AI-control (no forecast)	1809.70	9.7 %	—	4.81	0.21	−2.00

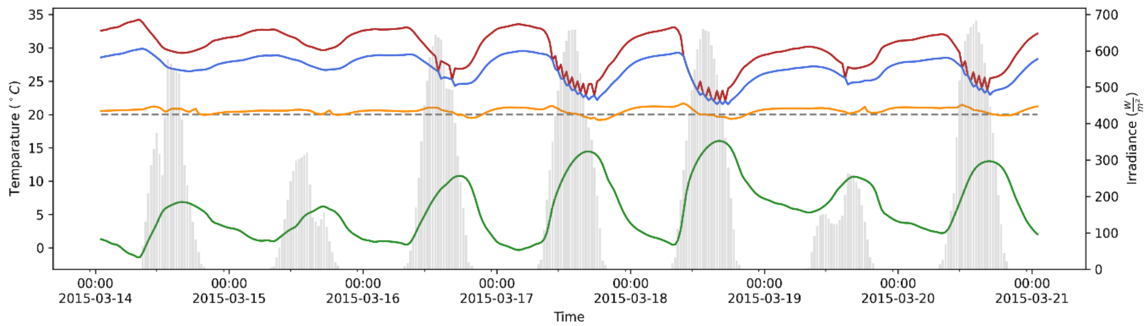

Figure 4 : Example of simulated rule-based (tuned heating curve) control for one-week HP operation (yellow: room temperature, red: HP supply temperature, blue: HP return temperature, green: ambient temperature, grey: internal gains due to irradiation).

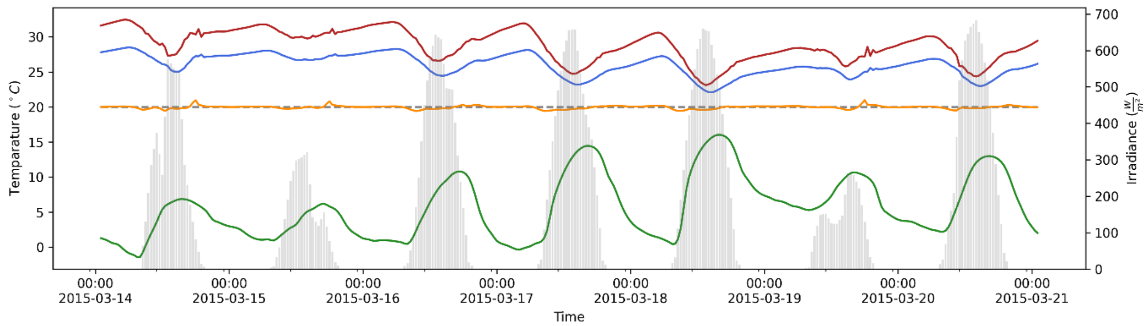

Figure 5 : Example of simulated AI-control for one-week HP operation (yellow: room temperature, red: HP supply temperature, blue: HP return temperature, green: ambient temperature, grey: internal gains due to irradiation).

R3

3.2. Field-test performance

Table 2 shows the results for (i) the one-week initial test and (ii, iii) the seasonal test.
During the baseline 2023/24 heating season, the heat pump has a seasonal COP of 3.95 and a mean absolute comfort deviation of 0.3 K. With the AI-retrofit controller installed, daily electricity consumption decreased by 8 %, the seasonal COP increased to 4.15 (+5 %) and the mean absolute comfort deviation fell from 0.3K

to 0.1 K. When days with higher average comfort deviations were removed, the performance gap increased further. Occupants reported noticeable improvement of the more stable comfort temperature. Figure 6 shows the daily mean COP of the AI-controlled HP operation compared to standard operation. The graph illustrates that the COP under AI control is higher on almost all days, indicating a more efficient conversion of electrical energy into heat. While both modes show day-to-day variations depending on outdoor temperature, the AI controller achieves a consistently higher and more stable efficiency throughout the observation period. It appears that the AI-based control achieves higher COP values mainly at milder outdoor temperatures, suggesting that its optimization strategy is particularly effective under part-load conditions. However, since the field sample covers only a limited time period and a single test site, this trend should be interpreted with caution.

Table 2: Comparison of KPIs for AI controller and standard heating curve controller for one-week test and seasonal test. Reference test sets were selected based on similar average ambient temperature. For the seasonal test (iii), days with a mean indoor temperature deviation above 0.25 K were excluded

	One-week AI (i)	Ref. (i)	AI (ii) 2024/25	Reference (ii)	AI (iii) 2024/25	Ref. (iii)
Mean ambient temp.	4.43 °C	4.57 °C	4.21 °C	4.21 °C	4.26 °C	4.26 °C
Mean comfort deviation	0.18 K	0.64 K	0.1 K	0.3 K	0.1 K*	0.1 K *
Mean COP	4.19 (+0.33, +9%)	3.86	4.15 (+0.2, +5%)	3.95	4.12 (+0.18, +5%)	3.94
Mean daily electr. cons.	24.4 kWh (-9%)	26.7 kWh	25.49kWh (-8%)	27.64 kWh	25.34kWh (-11%)	28.39 kWh

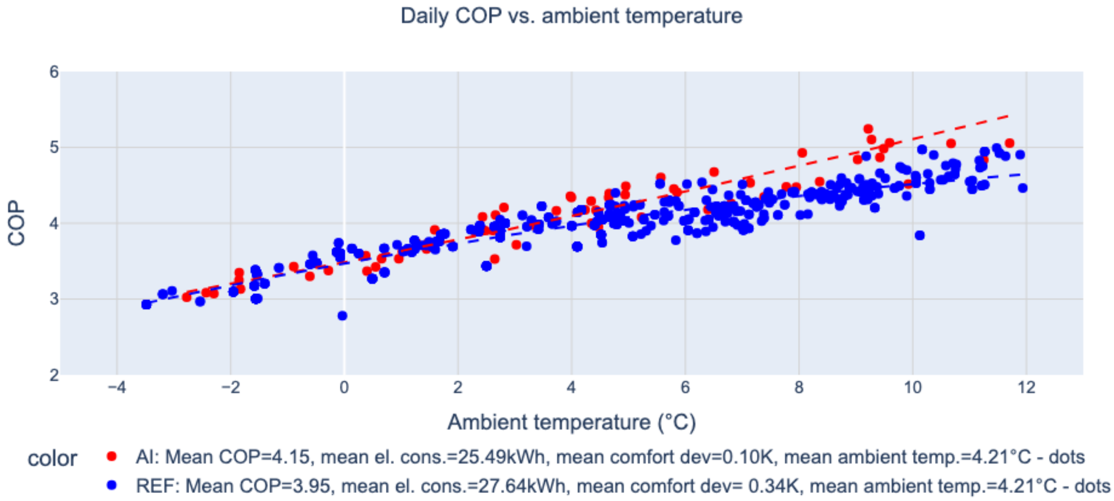

Figure 6 : Daily mean COPs of AI (red) vs. standard operation (blue) with fitted curve through all the coloured points.

4. Discussion

4.1. Comparison simulation and field test results

While comparability is difficult due to differing setups, the reported savings in the simulations tests (electricity consumption reduction by 2 – 15% depending on baselines and conditions, COP improvement of up to 0.3 points) are consistent with the field test results. Thus, the field trial confirmed the simulation findings under real operating conditions.

4.2. Benefits of predictive control

With the AI-retrofit controller installed, daily electricity consumption decreased to from 27.64 kWh to 25.49 kWh (–8 %). Over a 180-day heating season these improvements correspond to about 387 kWh of saved electricity and 23 kg of avoided CO_2 emissions (assuming 0.06 kg CO_2 per kWh of electricity in the German

grid). The control algorithm operated reliably on the embedded hardware, with an average computational time of a few milliseconds per optimisation and no connectivity to external cloud services.
The results demonstrate that accurate temperature forecasting combined with optimisation enables significant energy savings. By anticipating solar gains and occupancy patterns, the controller avoids unnecessary overheating and reduces compressor cycling. The Transformer architecture captures long-range dependencies in the thermal dynamics and outperforms simpler recurrent networks on our datasets. The cost function's weighting factors allow tuning between comfort and efficiency. In practice we found that moderate discomfort weights yield substantial energy savings with negligible comfort impacts.
The improvements in COP observed in both simulations and the field trial highlight that the energy savings are not simply due to reducing indoor temperatures. Instead, the controller operates the heat pump closer to its optimal operating point, avoiding high supply temperatures that diminish COP at mild outdoor conditions. The reduced mean absolute comfort deviation in the field trial indicates that the controller maintains or improves comfort despite the energy savings.
Further improvements are expected if the heat pump efficiency (i.e., electrical power consumption) is integrated into the objective function of the control algorithm. However, this was not yet implemented due to the lack of high-resolution real-time compressor power data.

4.3. Limitations and future work

Several limitations should be considered. First, the simulation models are simplified representations of real buildings and heat pump performance. They do not capture occupant behaviour variability or moisture dynamics. For instance, frosting and defrosting cycles of air-source heat pumps are not modelled, although these can significantly lower seasonal COP by increasing compressor workload and temporarily interrupting heating during humid, near-freezing conditions. Second, the field trial covers one heating season in a single house; additional trials across diverse climates and building types are needed to generalise the results. Third, the current implementation controls a single heating circuit. Extending the controller to multi-zone buildings with floor heating and multiple thermostats requires additional sensing and coordination.
Comparability of AI-enabled advanced HP controls between different simulation and field test remains limited due to differing setups, baselines and short trials. More long-term field trials in real, occupied buildings are needed to produce comparable results and verify robustness, comfort, and transferability across systems and climates.
Integration with renewable electricity and grid services also presents opportunities. By incorporating electricity price forecasts or grid-carbon intensity signals, the optimiser could schedule heat-pump operation to periods of low carbon intensity. To fully exploit such dynamic optimisation, the model would need to include the domestic hot-water tank, as it provides the thermal storage capacity required to shift operation in time. Finally, the system could learn occupant comfort preferences and allow manual overrides through a user interface. Ensuring reliability and ease of installation will be key for large-scale adoption.

5. Conclusions

This work demonstrated a proof-of-concept AI-driven retrofit controller for residential heat pumps. By connecting to standard 0–10 V or Modbus inputs, the controller can override manufacturer heating curves without modifying hardware. A lightweight Transformer model forecasts indoor temperature using existing sensor data, and a real-time optimiser selects the supply-water temperature to minimise a weighted sum of thermal discomfort and compressor energy. Simulations across nine archetype buildings show average electricity savings of up to 15 %, COP improvements up to 0.3 and significantly decreased comfort violations compared with static heating curves. A field trial in a renovated single-family house confirms an 8 - 11% reduction in daily electricity consumption and a 5 % increase in seasonal COP. These findings indicate that edge-AI controller retrofits can provide immediate and significant decarbonisation benefits across the installed heat-pump base. The presented edge-AI controllers demonstrated these energy savings by processing historical temperature and occupancy patterns to predict the ideal temperature path and dynamically adjust climate-control settings. These results indicate that machine-learning-based control can outperform static heating curves.

Acknowledgements

The authors acknowledge the financial support by the German Federal Ministry of Education and Research in the project 'AI4HP' (01IS21081A). We also thank the homeowners who participated in the field trial.

References

[1] Mastrucci, A., Boza-Kiss, B. & van Ruijven, B. Towards net-zero emissions in global residential heating and cooling: a global scenario analysis. Climatic Change 178, 85 (2025). https://doi.org/10.1007/s10584-025-03923-6

[2] Miara, M., Günther, D., Langner, R., & Helmling, S. (2014). Efficiency of heat pumps in real operating conditions. REHVA Journal, 2014, 7–12.

[3] Frison, L., Kleinstück, M., & Engelmann, P. (2019). Model-predictive control for testing energy flexible heat pump operation within a hardware-in-the-loop setting. Journal of Physics: Conference Series, 1343(1), 012068. https://doi.org/10.1088/1742-6596/1343/1/012068

[4] Stoffel, P., Berktold, M., Müller, D., 2024. "Real-life data-driven model predictive control for building energy systems: comparing different machine learning models," Energy and Buildings, 305, 113895. https://doi.org/10.1016/j.enbuild.2024.113895.

[5] Frison, L., Gölzhäuser, S., 2024. "Adaptive neural-network-based control approach for building energy control under changing environmental conditions," Proceedings of the 6th Annual Learning for Dynamics & Control Conference (L4DC), Oxford, UK, 15–17 July 2024. PMLR 242, 1741–1752.

[6] Maier, L., Brillert, J., Zanetti, E., Müller, D., 2024. "Approximating model predictive control strategies for heat pump systems applied to the building optimization testing framework (BOPTEST)." Journal of Building Performance Simulation 17(3), 338–360. 10.1080/19401493.2023.2280577.

[7] Dengiz, T., Kleinebrahm, M., 2024. "Imitation learning with artificial neural networks for demand response with a heuristic control approach for heat pumps," Energy and AI, 18, 100441. https://doi.org/10.1016/j.egyai.2024.100441.

[8] Du, Y., Zandi, H., Kotevska, O., Kurte, K., Munk, J., Amasyali, K., McKee, E., Li, F., 2021. "Intelligent multi-zone residential HVAC control strategy based on deep reinforcement learning." Applied Energy 281, 116117. 10.1016/j.apenergy.2020.116117.

[9] Svetozarević, B., Baumann, C., Muntwiler, S., Di Natale, L., Zeilinger, M. N., Heer, P., 2022. "Data-driven control of room temperature and bidirectional EV charging using deep reinforcement learning: Simulations and experiments." Applied Energy 307, 118127. 10.1016/j.apenergy.2021.118127.

[10] Montazeri, M., Remlinger, C., Bejar Haro, B., Heer, P., 2025. "Fully data-driven and modular building thermal control with physically consistent modeling," Applied Energy, 390, 125770. https://doi.org/10.1016/j.apenergy.2025.125770.

[11] Rohrer, T., Frison, L., Kaupenjohann, L., Scharf, K., & Hergenröther, E. (2023). Deep reinforcement learning for heat pump control. In Proceedings of the Science and Information Conference (pp. 459–471). Springer.

[12] Mulayim, O. B., Pergantis, E. N., Reyes Premer, L. D., Chen, B., Qu, G., Kircher, K. J., Bergés, M., 2025. "Comparative Field Deployment of Reinforcement Learning and Model Predictive Control for Residential HVAC," arXiv preprint arXiv:2510.01475.

[13] Zhang, B., Frison, L., Brox, T., Bödecker, J., 2024. "Constrained reinforcement learning for safe heat pump control," arXiv preprint arXiv:2409.19716. https://doi.org/10.48550/arXiv.2409.19716.

[14] Pergantis, E. N., Priyadarshan, Al Theeb, N., Dhillon, P., Ore, J. P., Ziviani, D., Groll, E. A., Kircher, K. J., 2024. "Field demonstration of predictive heating control for an all-electric house in a cold climate," Applied Energy, 360, 122820. (Author preprint: arXiv:2402.07032).

[15] Frison, L., Paul, S., Koller, T., Fischer, D., Frison, G., Boedecker, J., & Engelmann, P. (2020). Hardware-in-the-loop test of learning-based controllers for grid-supportive building heating operation. IFAC-PapersOnLine, 53(2), 17107–17112. https://doi.org/10.1016/j.ifacol.2020.12.059